

# FAULT DETECTION USING PALSAR-1/2 IMAGE DATA FOR GROUNDWATER ANALYSIS IN CENTRAL AND SOUTHWEST OF DJIBOUTI

Yessy Arvelyna<sup>1</sup>, Sawahiko Shimada<sup>2</sup>, \*Sergio Azael May Cuevas<sup>2</sup>, Fadoumo Ali Malow<sup>3</sup>

<sup>1</sup>Remote Sensing Technology Center of Japan, Japan

<sup>2</sup>Faculty of Regional Environment Science, Tokyo University of Agriculture, Japan

<sup>3</sup> The World Bank, Djibouti

\*Corresponding Author, Received: 14 Mar. 2022, Revised: 12 Jan. 2023, Accepted: 26 Feb. 2023

**ABSTRACT:** Fault mapping is done to observe the possibility of fault-driven groundwater flow into the fault systems. Fault detection analysis on PALSAR-1/2 data has been implemented through a series of adaptive and gradient filters to derive a Relief Image. This method was applied to delineate good-resolution faults distribution and to revise faults mapping derived from existing geology maps over Djibouti. Study areas are located in the central and southwest of Djibouti, where faults exist because of continental plate movements, contact of geological formation, and tectonics activities. Results show that the processed Relief Image could delineate the fault lines and remove artifacts from PALSAR-1/2 data. Furthermore, the Geology Scoring Index was introduced in this study to analyze the correlation of groundwater data with the geology setting of borehole sites such as geological formation, fault system from Relief Image, distance to rivershed, type of aquifer, etc. It is shown that the occurrence of fault systems possibly increases the groundwater volume of boreholes in study areas. The proposed study is useful to locate the potential area for groundwater resources in Djibouti.

**Keywords:** ALOS-2, PALSAR-2, Fault Detection, Groundwater Analysis, Djibouti.

## 1. INTRODUCTION

Djibouti is a country located in the region known as the Horn of Africa, sharing borders with Ethiopia, Eritrea and Somalia and facing the Aden Gulf, with a surface of around 23,200 km<sup>2</sup>. It has a low rainfall of approximately 130 mm/year due to its semi-arid and arid climate, which mostly evaporates to the air (83.5 %) and the rest flows on the ground surface (6 %), penetrates into the sub-surface (5.5 %) and sub-ground (5 %), forming renewable groundwater resources, estimated to be about 300 million m<sup>3</sup>/year [1]. For these arid conditions, groundwater is a very valuable water resource in the country.

In previous studies, thematic maps, such as lineament, lithology, soil, drainage density, elevation, etc., have been used to delineate groundwater potential zones [2, 3]. It was considered that the lineament density (km/km<sup>2</sup>), e.g., the presence of faults, was the parameter with more weight when estimating the groundwater potentiality [2], because it promotes groundwater movement.

In Djibouti, fractures in volcanic aquifers have been considered as the main water resource, as shown by the pumping test data, conducted on major basaltic series, e.g., the Stratiform series (3.4 Ma to 1 Ma) and the Dalha series (9 Ma to 3.4 1 25 Ma) with a thickness of more than 200 m [4]. In

addition, geochemical and isotopic surveys in the southwest of Djibouti showed a common evolutionary pattern of groundwater, i.e., a recharge from wadi-rivers flown into the alluvium layer, then circulated downward into the basalt layer through major faults and mixed with a more geochemically evolved groundwater [5]. Therefore, it is considered necessary to delineate the fault distribution, to locate areas with high possibility of groundwater resources. Previously, geology maps of Djibouti have been produced with fault lines digitized using satellite imagery of 15 m resolution [6]. To complement this information, faults were detected using the interpretation of bright and dark signatures of backscattering data on Synthetic Aperture Radar (SAR) image data, [7].

This study aims to delineate fault systems using open and free data products of PALSAR-1/2 (Phased Array type L-band Synthetic Aperture Radar) image data over Djibouti by analyzing fault distribution on a Relief Image processed using the gradient filter method. In addition, location of boreholes, groundwater data and geologic setting were selected as parameters to estimate the correlation between fault distribution and groundwater resource characteristics. Based on this correlation, the Scoring Index for Geology Setting Analysis of Borehole Site was proposed, to visualize those parameters and to map the potential area for groundwater. The proposed method can be

used to locate potential groundwater areas in Djibouti, with open data and limited field data.

This study is done under the project “Advanced and Sustainable Methods on Water Utilization Associated with Greening Potential Evaluation” aimed to create sustainable agropastoral practices in the Djibouti desert through developmental management of water resources, designated by the Tokyo University of Agriculture, Japan, from FY2018 for 5 years period [8].

## **2. RESEARCH SIGNIFICANCE**

The significance of this study is the estimation of groundwater location using the proposed Geological Scoring Index (GSI) obtained from the correlation with fault distribution derived using PALSAR-2 data, geological setting, and the analysis of existing borehole data in the study area.

## **3. DATA**

### **3.1. SAR Image Data**

SAR (Synthetic Aperture Radar) data has been widely used in volcanic and tectonic terrains. Because imaging radar is sensitive to changes in slope, rough-ground surface scatters higher radar signals on the front, while lower radar signals are backscattered on the back slope [7]. Thus, fault lines and their associated topographic scarps are emphasized by highlight (whitish feature) and shadow (blackish feature) on a SAR image [9]. In the SAR image, a thrust fault can be detected by different trends of underlying rocks, and strike-slip faults are often shown by aligned notches, shutter ridges, linear terraces and offset stream channels [7]. The advantage of using a SAR image is that a radar signal can penetrate clouds and observe the ground surface night and day; thus, it can produce image data without cloud problems. Radar backscatters, derived from satellite observation with high look angle, can produce an extreme topographic distortion, hence, it needs geometric terrain correction to produce good image data. The processed PALSAR-1/2 data in this study are described below.

#### *3.1.1. PALSAR-1 ASF RT1 data*

PALSAR-1 sensor was aboard on Japanese ALOS (Advanced Land Observing Satellite) for land observation using L-band frequency with the main objective to contribute to cartography, regional observation, disaster monitoring, and resource surveying [10]. The Alaska Satellite Facility (ASF) has processed Radiometrically Terrain Corrected (RTC) ALOS PALSAR products which are accessible to users on GeoTIFF format

since 2014 [11].

The PALSAR RTC product has been adjusted for geometry terrain by correcting geometric distortions that lead to geolocation error, and for radiometric correction by removing topography influence on backscatter values [12]. This study selected 8 scenes of RT1 high-resolution product which has gamma naught power on pixel data with 12.5 m resolution over the Djibouti region. For the Djibouti region, the geometric correction uses SRTM GL1 DEM (Digital Elevation Model) data up-sampled 30-m mapping function to 12.5 m mapping function. The RT1 image data can be downloaded from ASF Data Portal under the Product License Agreement and Citation [13].

#### *3.1.2. PALSAR-2 global mosaic data*

Starting in 2014, the ALOS-2 PALSAR-2 data is the continuation of the PALSAR-1 program that ended in 2011. The PALSAR-2 Global Mosaic Data is a seamless mosaic of the backscattering coefficients of PALSAR-2 image with 25 m resolution within 10x10 degrees in latitude and longitude released by JAXA (Japan Aerospace Exploration Agency) in 2018. Geometric distortion correction (ortho-rectification) and topographic effect on image intensity (slope correction) are applied [14]. The temporal interval of the mosaic is generally 1 year. This data is aimed at understanding and responding to global environmental changes such as global warming and loss of biodiversity, timely assessment of deforestation, and forest degradation. Users can access free and open datasets with registration on JAXA site under specific JAXA's Terms of Use of Research Data [15]. This study has acquired 4 scenes of PALSAR-2 Global Mosaic data over the Djibouti region.

### **3.2 Geology Map**

The geology map over Djibouti (Fig.1) [16][17] is used to observe the geological formation of boreholes, e.g., basaltic or sedimentary formation, the distance to rivershed (wadi), type of nearby fault system and type of aquifer that correlates with the production level of groundwater.

### **3.3 Borehole Data**

For this study a collection of past borehole data in Djibouti, obtained by a FAO project, was analyzed [18]. The spatial distribution of borehole sites and their groundwater data such as discharge, conductivity, depth and elevation, are used to analyze the impact of fault distribution on groundwater resources. The description of borehole data for the target area is noted below.

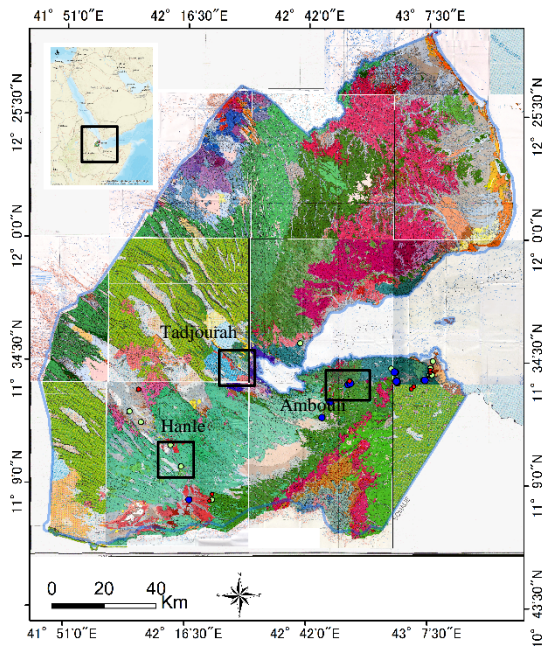


Fig. 1 Geology map of Djibouti and study area

## 4. STUDY AREA

### 4.1. Ambouli Watershed

The Ambouli watershed is located in the southwest of Djibouti city, whose main water resource came from the wadi Ambouli. The aquifers at the Ambouli watershed are mainly composed of volcanic aquifers and part of sedimentary aquifers. Normal faults with a throw of less than 20 m and faults without a throw are mostly observed in NW-SE, W-E, and NE-SW directions [17]. About 58 boreholes are distributed in the Ambouli watershed and from these, 36 boreholes with groundwater discharge data were analyzed.

### 4.2. Hanle Watershed

The Hanle watershed is stretched from the west into the southwest of Djibouti. The aquifers in the Hanle watershed are mainly composed of sedimentary aquifers and regional volcanic aquifers. In this region, the formation of older basalt of the Stratoid series ( $\beta D$ ), middle Stratoid basalts of the Afar ( $\beta SI I$ ), and the Dalha basaltic series ( $\beta D$ ) are widely covered and in some parts are overlaid by younger sedimentary layers of alluvial deposits ( $Qa$ ,  $A3 - A5$ ) observed from the north into the south part region of the watershed [17] with depth about 100 m [18]. From 30 boreholes located in the Hanle watershed, only 9 boreholes, which have groundwater discharge data, were analyzed in this study.

### 4.3. Tadjourah Region

In the Tadjourah region, complex fault systems are observed, such as in the Asal rift zone, the central part of Djibouti. The aquifers in this region are mainly composed of volcanic aquifers and minor sedimentary aquifers. The geology setting shows complex layers from the basaltic series of Dalha ( $\beta D$ ) on the north side, basalts of external margins of the Asal ( $\beta G1$ , recent Quaternary) in the central part, initial basalt series of the opening of the gulf of Tadjourah ( $\beta i$ ) along the coastal area and in between overlaid with recent sedimentary formations ( $Qa$ ) from upper Pliocene to middle Pleistocene era [6]. Normal faults and faults without throw are observed mostly in NW-SE and NE-SW directions, respectively (Fig.1). Twenty boreholes are distributed in this region.

## 5. IMAGE PROCESSING METHOD

### 5.1. Preprocessing

The PALSAR-1/2 data were re-projected to have the same datum and projection, e.g., WGS 1984 Lat/Long. The PALSAR-1 ASF RT1 data uses WGS 1984 datum and UTM 37N projection and the PALSAR-2 global mosaic data uses WGS1984 latitude/longitude. Therefore, the RT1 data is re-projected into WGS 1984 Lat/Long. The DN pixel value of backscattering of RT1 image (HH or HV band) was converted into gamma naught values in dB (decibel) using the following equation [11],

$$dB = 10 * \text{Log}_{10}(\text{sqrt}(\text{DN}))^8 \quad (1)$$

The PALSAR-2 global mosaic data products were stored as the DN number in unsigned 16 bit and the conversion into gamma naught in dB was done using the following equation [15]:

$$dB = 10 * \text{Log}_{10} \langle \text{DN}^2 \rangle + CF^{12} \quad (2)$$

Where, CF is a calibration factor (value is -83 dB for PALSAR-1 mosaic data), and  $\langle \rangle$  is the ensemble averaging.

Since SAR data is filled with speckle noise due to the interferences during signal transmission [20], adaptive filters, such as Enhanced Lee Filter, etc., were applied on PALSAR-1/2 data to reduce speckle noise on the image. Adaptive filters use the standard deviation of pixels within a moving window/box to calculate new pixel values. Enhanced Lee filter was used to reduce speckles in SAR images while preserving texture information [21]. The filtering process utilized the Damping Factor, which is the exponential damping in the weighted average for the heterogeneous class, where larger damping produces less averaging. "Homogenous" is the pixel value replaced by the average of the filter window and "Heterogeneous"

is the pixel value replaced by a weighted average.

## 5.2. Fault Detection Analysis Using the Relief Image

Since the fault lines on SAR image are associated with the dark-light transition, this feature contains edges that possess gradients with a large magnitude on the X-Y plane [22]. Therefore, it can be emphasized using gradient filters. In this study, fault distribution was delineated from the processed Relief image composed by applying a gradient filter on ortho-rectified PALSAR-1/2 image data to emphasize the relief features of fault lines. On ENVI ver. 5.5.3, this process was done by applying Convolution High Pass Filter with 3x3 Kernel Size on X and Y direction by applying Kernel in X direction: [-1, 0, 1]; [-2, 0, 2]; [-1, 0, 1] and Y direction: [1, 2, 1]; [0, 0, 0]; [-1, -2, -1].

Then, the Relief image was derived by composing the X and Y direction gradient filtered image (b1+b2), such as the Band Math of ENVI or the raster tool of ArcMap. Fault detection analysis was done by overlaying the Relief image derived from gradient filtering of PALSAR-1/2 data on the geology map over Djibouti using ArcMap ver.10.6 with a transparency setting of about 45%. The correlation of the fault line from the geology map over the study area and the Relief image was observed under an image scale from 1:30,000 or higher.

## 5.3. Scoring Index for Geology Setting Analysis of Borehole Site

The correlation between the groundwater volume from the borehole and the geology setting of the borehole site is analyzed using the Geology Scoring Index which is designed according to the information derived from the geology map over Djibouti, e.g., basaltic or sedimentary formation, the distance to rivershed (wadi), type of nearby fault system and type of aquifer that correlate with the production level of groundwater (Table 1), so it is expected that the higher the index value in any group, the bigger the groundwater volume will be.

In Group I, Geology formation, two indexes were proposed for classification, consisting of Sedimentary formation (SedF\_i) and Basaltic formation (BasF\_i), which are widely distributed in study areas. The infiltration of groundwater mainly occurs in the sedimentary formation in the wadi beds [1]. The sedimentary formations along main wadi beds at study areas are generally filled with heterogeneous sediments with coarse materials, such as gravels, sands, shales and fine sediments and intrusion of basaltic formation [5]. With the assumption that coarser material of sedimentary formation is capable of absorbing more runoff water, the index score for SedF\_i is given 2 and BasF\_i is 1.

Table 1. Geology Scoring Index (GSI) for borehole sites

Group	No	Class	Index Name	I	Category
I. Geological formation	1	Sedimentary formation	SedF_i	2	Capacity to absorb water
	2	Basaltic formation	BasF_i	1	
II. Rivershed	3	Dry rivershed	Rv_i	2	Distance to rivershed
	4	Near dry rivershed	Rv_i	1	
III. Fault	5	Along major fault	F_i	3	Correlation to fault
	6	Along fault	F_i	2	
	7	Possibly along fault	F_i	1	
	8	Local sedimentary aquifer	SedAq_i	2	
IV. Aquifer type	9	Local volcanic aquifer	VolAq_i	1.5	Capacity to absorb water
	10	Regional volcanic aquifer	VolAq_i	1	

In Group II, Rivershed, the index score Rv\_i is proposed by considering the distance of borehole to rivershed, since the hydrogeological process of surface runoff flow and water infiltration mostly over the wadi river sheds. The borehole located along the rivershed is given the highest score Rv\_i=2 and for the area nearby rivershed Rv\_i=1.

The fault system is considered as one important factor in groundwater circulation, as mentioned in [5], where the recharge from wadi-rivers to the alluvium and a downward circulation to the basalt through major faults, combined with a mixing with a more geochemically evolved groundwater. Thus, the location into a major fault system is designed with a higher index score and smaller fault with lower score for Group III, Fault.

Analysis of the data from pumping tests was conducted since the 1960s in the sedimentary and volcanic aquifers in the Republic of Djibouti [4]. It showed that measured transmissivity data collected on the sedimentary aquifers range between very low ( $T=0.4 \text{ m}^2 \text{ h}^{-1}$ ) and relatively high values ( $T=163 \text{ m}^2 \text{ h}^{-1}$ ). These formations are quite heterogeneous and the variable clay content in sediments and also to hydrothermal effects as observed in the field is the reason behind the extended transmissivity range. The material contents formed in local sedimentary aquifer (SedAq\_i) is assumed to have higher water infiltration rates than local/regional volcanic aquifer (VolAq\_i). The borehole data in the study area, i.e., groundwater volume and depth profile, borehole elevation, etc., were also analyzed and visually compared using graphs.



## 6. DISCUSSION AND ANALYSIS

### 6.1. Fault Detection Analysis

The proposed method of the Relief image by applying a gradient filter on PALSAR-1/2 image data could delineate the fault system in the study area. This method enhanced the difference of backscattering data from the ground surface occurred by the fault system retrieved as higher backscattering coefficients. The Relief Image shows that fault lines and dry rivers are associated with rugged features on image (Fig.2, top), where the fault line appears as straight lines and the river system as curved lines.

The overlay with the geology map (Fig. 2, bottom) shows that the extracted fault lines from the Relief Image are consistent with fault lines from the geological map. Normal faults such as in the Asal rift zone, appear as a straight and deep relief. Additional fault lines were delineated from the Relief Image which added to the fault system distribution from the geology map. The source data for the Relief Image, e.g., orthorectified image data of PALSAR-1 RT1 and PALSAR-2 Global Mosaic data, produced an accurate position of fault lines from the Relief Image, which improved the fault lines distribution from the geology map over Djibouti.

### 6.2. Boreholes Data Analysis

The result of the Geology Scoring Index (GSI) of boreholes introduced by this study (Table 1) shows the correlation of geology setting of borehole sites and groundwater resources in the study area (Fig. 4). It is revealed that the boreholes in study areas are mostly located at or near dry riverbed of wadi (blue) and more than half of borehole sites are located at the fault systems (orange).

At the Ambouli watershed, a higher conductivity level with a range between 2850 and 5300  $\mu\text{S}/\text{cm}$ , is shown for borehole data located at basaltic formation (RG1-RG3, RG5), in comparison with boreholes data at sedimentary formation (E1-E5) with range 2240 - 3625  $\mu\text{S}/\text{cm}$  (Fig.3.d). At the Hanle watershed, the borehole data (Dikhil6, Dikhil11) from volcanic aquifers at basaltic formation in fault regions also show a high conductivity level of 1950 – 2900  $\mu\text{S}/\text{cm}$ . High conductivity shows mineralization of groundwater from water-rocks interaction in basalt formations. In Djibouti the recharge of basaltic aquifers is related to downward circulation of surface water into deeper basalt layers through major faults [5]. For borehole sites closer to Djibouti city, higher conductivity levels are retrieved. The highest conductivity is shown at the EDD borehole located in Djibouti city.

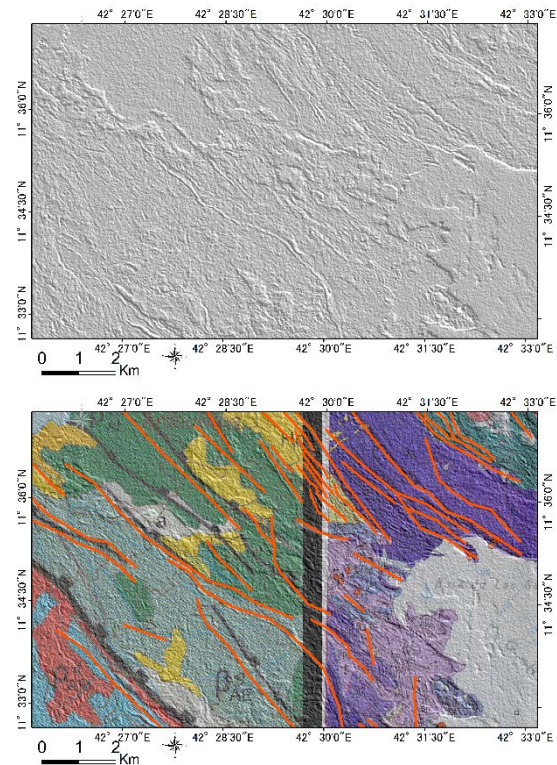


Fig. 2 Processed the Relief image derived from PALSAR-1 ASF RT1 data at the Asal rift zone (top), which is overlaid with the geology map (bottom) to extract fault lines (orange).

This result possibly shows the salinization of groundwater. The observed conductivity levels of groundwater of some boreholes exceed the WHO standard for drinking water ( $< 1,500 \mu\text{S}/\text{cm}$ ) and FAO standard for water quality agriculture, i.e.  $>700 \mu\text{S}/\text{cm}$  is slightly restricted to use and  $>3000 \mu\text{S}/\text{cm}$  is strictly restricted to use and assumed inadequate for irrigation from past field survey in Dikhil region [23].

The occurrence of a large fault system possibly increases the groundwater resource as shown at PK20-8 ( $Q=30 \text{ m}^3/\text{h}$ ) and PK-201 ( $Q=41 \text{ m}^3/\text{h}$ ) boreholes, which are located in a fault region, in comparison with borehole sites without the impact of the fault system, such as Chabelley-1 and Chabelley-2 ( $Q=6 - 20 \text{ m}^3/\text{h}$ ) in the Ambouli watershed (Fig. 3). Those boreholes are located about in the same elevation and depth profile (150 - 157 m). The borehole data of N-Goubet at an elevation of 183 m in the Tadjourah region, e.g., depth profile (183 m), low groundwater discharge ( $13.33 \text{ m}^3/\text{h}$ ) and the highest NS data (122.76 m) show the possibility of high fluctuation of the groundwater in faults region. High fluctuation of the NS data is also shown for boreholes data at the Hanle watershed (Kouri Koma III, Liliya Iburi Cheikati, Dikhil 6 and Dikhil 8) with deep depth profile (41 – 120 m), high elevation (184 – 474 m) and low discharge ( $2.2 - 30 \text{ m}^3/\text{h}$ ).

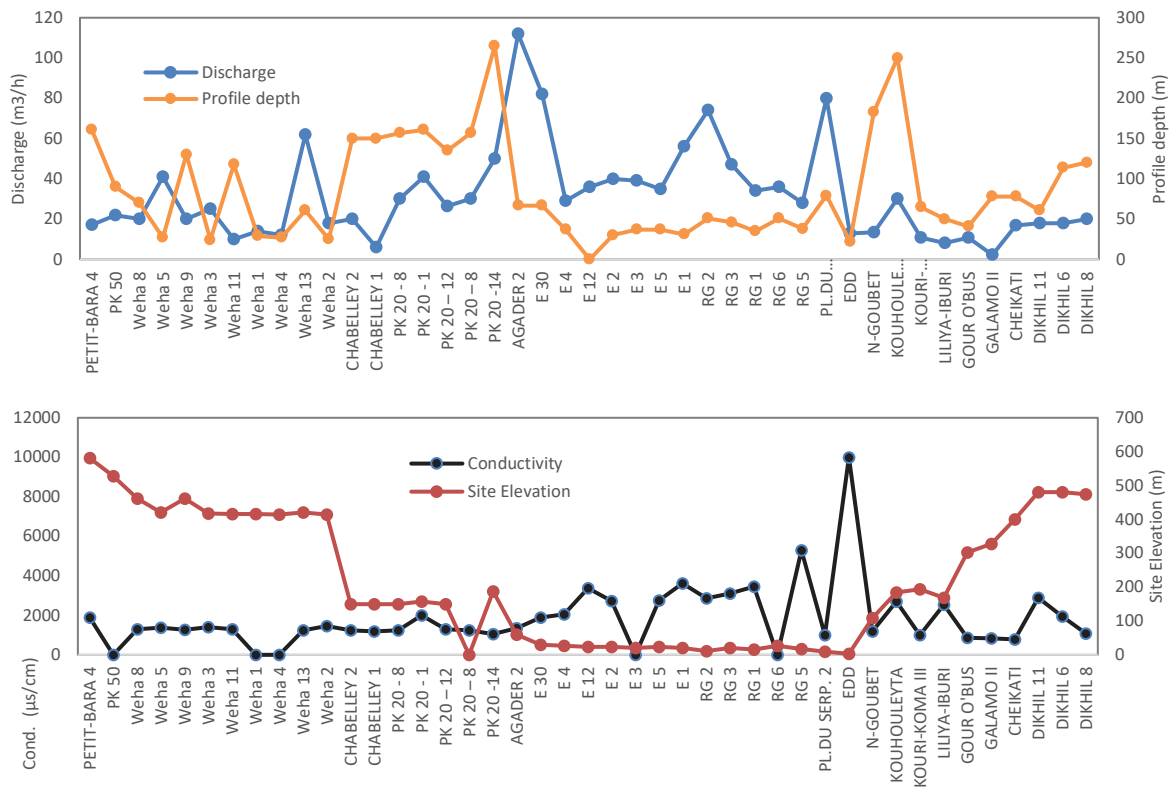


Fig. 3 Borehole data for study area: a) groundwater discharge per hour (Q); b) depth profile (m); c) conductivity ( $\mu\text{s}/\text{cm}$ ); and d) elevation (Z in m).

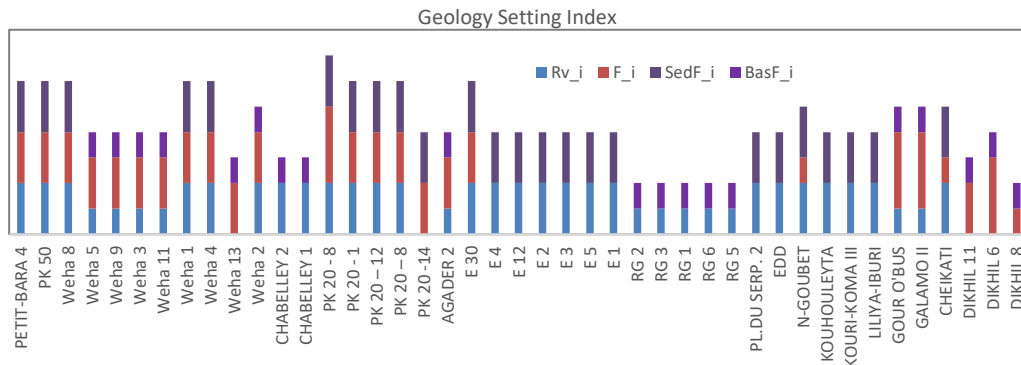


Fig. 4 Geology Setting Index for borehole sites introduced by this study

These results correlate with past studies that show the groundwater discharges in faults region increase linearly with the width and the number of fractures (faults) and decrease linearly with the increase in depth [24] and the magnitude of fluctuation increases to depth [25].

## 7. CONCLUSION

This study demonstrates that the proposed application of the Relief Image for fault detection using PALSAR-1/2 image data and the Geology Scoring Index analysis is useful to locate an area with a high possibility of groundwater resources. By evaluating the correlation between the geology

setting of borehole sites, e.g., geological formation, the occurrence of the fault system, aquifer type, etc. with borehole data, i.e. groundwater discharge, conductivity, depth profile, etc., potential sites for groundwater resources can be mapped. In study areas, potential groundwater resources are located in or near dry rivershed (wadi), sedimentary aquifers, and regions where fault systems exist. From the observation of the study area in the southwest and central of Djibouti, the fault regions in the western part (i.e., site of Weha 3, Weha 5, Weha 13) and the north part (PK 20-8, PK 20-1, PK 20-12) of the Ambouli watershed and the southwest of Djibouti city (site of Agader 2) show good potential of groundwater for irrigation and drinking

water. At these regions, the groundwater discharge ranges between 25 - 62 m<sup>3</sup>/h, the depth profile of boreholes 24 – 67 m, and the conductivity of borehole data below 1500 µS/cm.

Future application of this methodology could be used to locate potential areas for groundwater in Djibouti, where new groundwater stations could be established to support sustainable agropastoral practices in Djibouti

## 8. ACKNOWLEDGMENTS

This study acknowledged the copyright notice for ALOS PALSAR RTC © NASA [2006-2007], including material © JAXA, METI [2006-2007]. The PALSAR-2 Global Mosaic data have been provided by the Japan Aerospace Exploration Agency. The copyright of the Relief image and fault analysis products (including the Geology Setting Index analysis) derived from PALSAR-1/2 data over Djibouti is belong to RESTEC and the usage is granted to the Tokyo University of Agriculture/ SATREPS JST/JICA project through “Fault detection analysis using PALSAR-1/2 image data throughout Djibouti” project in FY2020.

## REFERENCES

- [1] Malow, F. A., Development of a 3D Water Flow Modelling based on Scarce Data for Arid Land Water Resources Management: Case Study of Ambouli and Kourtimalei Watersheds in Djibouti, Ph.D. Thesis, Tokyo University of Agriculture, Tokyo, Japan, 2018, pp.22.
- [2] Saifudding, M.F.U., Ash'aari, Z. H., Aris, A.Z, and Kusin, F.M, A Hybrid GIS and Knowledge-driven Approach for Water Resources Potential Zonation, International Journal of GEOMATE, July., 2021, Vol.21, Issue 83, pp.56-64.
- [3] Mogaji K.A., Lim H.S., and Abdullah K., Regional Prediction of Groundwater Potential Mapping in a Multifaceted Geology Terrain using GIS-based Dempster-Shafer Model. Arabian Journal of Geosciences, Vol. 8, Issue 5, 2014, pp. 3235–3258.
- [4] Jalludin, M. and Razack, M., Analysis of Pumping Tests, with Regard to Tectonics, Hydrothermal Effects and Weathering, for Fractured Dalha and Stratiform Basalts, Republic of Djibouti, Journal of Hydrology, Vol. 155, 1994, pp.237–250.
- [5] Awaleh, M. O., Baudron, P., Soubaneh, Y. D., Boschetti, T., Hoch, F. B., Egueh, N. M., Mohamed, J., Dabar, O. A., Masse Dufresne, J., and Gassani, J., Recharge, Groundwater Flow Pattern and Contamination Processes in an Arid Volcanic Area: Insights from Isotopic and Geochemical Tracers (Bara Aquifer System, Republic of Djibouti), Journal of Geochemical Exploration, Vol. 175, 2017, pp.82–98.
- [6] CERD, Geological map of the Republic of Djibouti, 1:200,000, Centre d'Etude et de Recherche de Djibouti, Djibouti, 2015.
- [7] Ford, J., Blom, R., Coloman, J., J.R., Farr, T., J.J, P., Pohn, H., and Jr., F. S., Radar Geology, in Henderson, F M, and Lewis, A J., Principles and Applications of Imaging Radar. Manual of Remote Sensing: 3rd ed., Vol. 2, 2013, pp.525-526.
- [8] JST, Advanced and Sustainable Methods on Water Utilization Associated with Greening Potential Evaluation, JST, 2018. [https://www.jst.go.jp/global/english/kadai/h3002\\_djibouti.html](https://www.jst.go.jp/global/english/kadai/h3002_djibouti.html).
- [9] Sabins, F. F. J., Remote sensing: Principles and Interpretation, Freeman and Co, New York, 2nd ed., 1987, pp.423.
- [10] JAXA, ALOS Data Users Handbook - Revision C, Earth Observation Research and Application Center, Japan Aerospace Exploration Agency, 2018, pp.2. [https://www.eorc.jaxa.jp/ALOS/en/doc/fdata/ALOS\\_HB\\_RevC\\_EN.pdf](https://www.eorc.jaxa.jp/ALOS/en/doc/fdata/ALOS_HB_RevC_EN.pdf).
- [11] ASF, ASF Radiometrically Terrain Corrected ALOS PALSAR Products - Product Guide, The Alaska Satellite Facility, Revision 1.2, 2015, pp.9.
- [12] ASF, View Radiometrically Terrain Corrected (RTC) Images in QGIS, The Alaska Satellite Facility, 2018. [https://asf.alaska.edu/wp-content/uploads/2019/02/view\\_rtc\\_in\\_qgis\\_v5.2.pdf](https://asf.alaska.edu/wp-content/uploads/2019/02/view_rtc_in_qgis_v5.2.pdf).
- [13] ASF, ALOS PALSAR – Terms and Conditions, 2021. <https://asf.alaska.edu/data-sets/sar-data-sets/alos-palsar/alos-palsar-terms-and-conditions>, Accessed: 2021-10-04.
- [14] JAXA, ALOS Data Users Handbook - Revision C, Earth Observation Research and Application Center, Japan Aerospace Exploration Agency, 2008. [https://www.eorc.jaxa.jp/ALOS/en/doc/fdata/ALOS\\_HB\\_RevC\\_EN.pdf](https://www.eorc.jaxa.jp/ALOS/en/doc/fdata/ALOS_HB_RevC_EN.pdf).
- [15] JAXA, Global PALSAR-2/PALSAR/JERS-1 Mosaic and Forest/Non-forest Map (FNF) - Dataset Description, Japan Aerospace Exploration Agency, 2019. [https://www.eorc.jaxa.jp/ALOS/en/palsar\\_fnf/DatasetDescription\\_PALSAR2\\_Mosaic\\_FNF\\_revI.pdf](https://www.eorc.jaxa.jp/ALOS/en/palsar_fnf/DatasetDescription_PALSAR2_Mosaic_FNF_revI.pdf).
- [16] ISERST, Carte Géologique de la République de Djibouti a 1:100,000, ORSTOM, Office de la Recherche Scientifique et Technique Outre Mer, Paris, France, 1983, 1985, 1986, 1987,

- 1995.
- [17] CERD, Geological map of the Republic of Djibouti, 1:200,000, Centre d'Etude et de Recherche de Djibouti, Djibouti, 2015.
- [18] Maudho, A., Water Resource Management in the Republic of Djibouti, FAO, Rural Hydraulic Directorate's Database Study Report, 2018.
- [19] JICA, Information Gathering and Confirmation Survey (Geophysical Exploration) for Djibouti Geothermal Development, 2015. [https://www.jst.go.jp/global/english/kadai/h3002\\_djibouti.html](https://www.jst.go.jp/global/english/kadai/h3002_djibouti.html), (in Japanese).
- [20] Skolnik, M. I., Introduction to Radar Systems, McGraw-Hill, Inc., 2nd ed., 1981, pp.537.
- [21] Lopes, A., Touzi, R., and Nezry, E., Adaptive Speckle Filters and Scene Heterogeneity, IEEE Transactions on Geoscience and Remote Sensing, Vol. 28, 1990, pp.992–1000.
- [22] Duda, R. O. and Hart, P. E., Pattern Classification and Scene Analysis, A Wiley-Interscience Publication, 1973, pp.268.
- [23] JICA, The Republic of Djibouti, the Master Plan Study for Sustainable Irrigation and Farming in Southern Djibouti, Final Report, 2014.
- [24] Basak, P., Lekha, K. R., and Prasad, P., Flow through Fractured Rocks: A Field Correlation between Fracture Parameters and Yield, in Workshop on Water Management: India's Groundwater Challenge, Ahmedabad, India, 1993.
- [25] Moench, M., Burke, J., and Moench, Y., Rethinking the Approach to Groundwater and Food Security, Water Reports, Food and Agriculture Organization of the United Nations, Rome, Vol.24, 2003, pp.40.

---

Copyright © Int. J. of GEOMATE All rights reserved, including making copies unless permission is obtained from the copyright proprietors.

---